DOI: 10.1021/ma100943t

Macromolecules
ARTICLE

Enhanced Performance of Bulk Heterojunction Solar Cells Using Novel Alternating Phenylenevinylene Copolymers of Low Band Gap with Cyanovinylene 4-Nitrophenyls

J. A. Mikroyannidis,*,† A. N. Kabanakis,† P. Balraju,‡,⊥ and G. D. Sharma*,‡,§

†*Chemical Technology Laboratory, Department of Chemistry, University of Patras, GR-26500 Patras, Greece,* ‡*Physics Department, Molecular Electronic and Optoelectronic Device Laboratory JNV University, Jodhpur (Raj.) 342005, India,* §*Jaipur Engineering College, Kukas, Jaipur (Raj.), India, and* ⊥*Molecular Electronics Laboratory JNCASR, Bangalore, India*

Received April 28, 2010; Revised Manuscript Received May 27, 2010

ABSTRACT: Two novel low band gap soluble copolymers, **P1** and **P2**, were synthesized and characterized. **P1** consisted of alternating dihexyloxyphenylene and α-[[4-(diphenylamino)phenyl]methylene]-4-nitro-benzeneacetonitrile. **P2** consisted of alternating dihexyloxyphenylene and α,α′-[(1,4-phenylene)dimethylidyne]bis(αZ,α′Z)-4-nitrobenzeneacetonitrile. These copolymers showed broad absorption curves with long-wavelength absorption maximum around 620 nm and optical band of 1.68 and 1.64 eV for **P1** and **P2**, respectively. Both **P1** and **P2** were blended with PCBM to study the photovoltaic response of bulk heterojunction (BHJ) solar cells. The highest occupied molecular orbital (HOMO) and lowest unoccupied molecular orbital (LUMO) levels of both **P1** and **P2** are well aligned with those of PCBM acceptor. This allows efficient photoinduced charge transfer and high open circuit voltage, leading to an overall power conversion efficiency (PCE) of 3.15% and 2.60% for the as cast **P1**:PCBM- and **P2**:PCBM-based devices, respectively. The PCE of the devices has been further improved up to 4.06% and 3.35% for the devices based on thermally annealed **P1**:PCBM and **P2**:PCBM blends, respectively.

Introduction

Organic solar cells using conjugated molecular materials have become increasingly feasible through the development of BHJ structures based on intimate blends of polymeric donors and soluble fullerene acceptors,[1−4] where efficient exciton separation is enabled by a large-area donor−acceptor interface.[5,6] The attractive features of this type of solar cell include the ease of solution-processing, low costs, light weight, and the potential application in flexible large-area devices.[7,8] So far, such devices based on polymer/fullerene blends have achieved high PCEs of more than 6%.[9−12]

In order to further improve the efficiency of BHJ polymer solar cells, the research is focused on the synthesis of new polymers. From the materials perspective, these donor polymers should not only have a low band gap (to increase the short circuit current, J_{sc}) but also bear a low energy level of the highest occupied molecular orbital (HOMO) (to improve the open circuit voltage, V_{oc}).[13] Typically, a low band gap polymer is designed via a "donor−acceptor" (D−A) approach, which is to incorporate electron-rich and electron-deficient moieties in the polymer backbone. The low band gap is mainly caused by the intramolecular charge transfer between donor and acceptor units.[14] In D−A copolymer, the electron unit provides a deeper HOMO level, whereas electron acceptor is used to tune the electronic bang gap.[10] In fact, several low band gap polymers have been demonstrated with decent efficiencies (3−6%) when they were blended with PCBM or [6,6]-phenyl C70-butyric acid methyl ester (PC70BM) in typical BHJ devices.[15−35] For example, PCDTBT, a low band gap polymer synthesized from a copolymerization of alkylated carbazole and 4,7-di-2-thienyl-2,1,3-benzothiadiazole (DTBT) recently demonstrated a record high efficiency of 6.1% when it was blended in a BHJ composite with PC70BM.[24]

Among conjugated polymers, poly(*p*-phenylenevinylene) (PPV) and its derivatives have been at the center of focus. For the applications in polymer solar cells (PSCs), PPVs[36] and polythiophenes (PTs)[37] have attracted much attention due to their good film-forming and optical properties. Up to now, the PSCs based on a blend of PPVs or PTs and PCBM have exhibited PCE over 3%[38] and 6%,[39,34] respectively. Recently, a PCE about 7.4% has been achieved from PTB7/PC71BM solar cell devices.[40] However, the PCE of the PSCs is still low, which is mainly suffered from the narrow absorption band and the low charge carrier mobility of the π-conjugated polymers. To fabricate high-efficiency solar cells, the promising conjugated polymers should possess a broader absorption to enlarge absorption spectrum range and higher charge carrier mobility to reduce charge recombination and increase the photocurrent.

Various low band gap small molecules and polymers carrying cyanovinylene 4-nitrophenyls have been synthesized in our laboratory and used for BHJ solar cells[41] and dye-sensitized solar cells[42] with enhanced efficiency. In continuation of this research line, herein we synthesized two novel alternating phenylenevinylene copolymers **P1** and **P2** with the D−A structure. Particularly, both copolymers contained the hexyloxyphenylene as one constructional unit. The other constructional unit was the α-[[4-(diphenylamino)phenyl]methylene]-4-nitrobenzeneacetonitrile for **P1** and α,α′-[(1,4-phenylene)dimethylidyne]bis(αZ,α′Z)-4-nitrobenzeneacetonitrile for **P2**. The hexyloxy side groups rendered both copolymers soluble in common organic solvents. The presence of triphenylamine in **P1** is expected to enhance the hole

*Corresponding authors: tel +30 2610 997115, fax +30 2610 997118, e-mail mikroyan@chemistry.upatras.gr (J.A.M.); tel 91-0291-2720857, fax 91-0291-2720856, e-mail sharmagd_in@yahoo.com (G.D.S.).

 Published on Web 06/10/2010

mobility of this copolymer. A literature survey revealed that the α-[[4-(diphenylamino)phenyl]methylene]-4-nitrobenzeneacetonitrile unit has been utilized as nonlinear chromophore.[43] In addition, this unit, but without the nitro group, has been utilized for electrophotographic photoreceptor and electrochromic display devices.[44] Finally, an alternating phenylenevinylene copolymer similar to **P2**, but without the nitro groups, has been reported in a Chinese patent as electroluminescent photovoltaic (PV) material.[45] The optical, electrochemical, and electrical properties of copolymers **P1** and **P2** and their performance for PV devices are reported. The overall PCE of the devices based on the as cast **P1**:PCBM and **P2**:PCBM is about 3.15% and 2.60%, respectively. The higher value of PCE for **P1**:PCBM has been attributed to (i) the higher difference in the LUMO levels between **P1** and PCBM as compared to the difference in LUMO levels of **P2** and PCBM and (ii) the relatively higher value of the hole mobility for **P1**. When thermally annealed **P1**:PCBM and **P2**:PCBM active layers are used in the device, the PCE was further increased up to 4.06% and 3.35%, respectively. This enhanced PCE with thermally annealed blends has been related to the increase in both crystallinity of donor material in blend and hole mobility.

On the other hand, in order to improve organic photovoltaic cells, our efforts should not be solely focused in enhancing their power conversion efficiency as it will be proved pointless without addressing their weaknesses, i.e., poor UV-light stability and reduced lifetime. These limiting factors must be taken seriously into account as they are responsible for the loss of the electronic properties of the material used in the active layer after a very short time in use conditions. Several recent reports concerning the study of lifetime of the organic devices, during storage both in the dark[46] and under illumination,[47,48] have been published. The degradation of organic solar cells may be caused by several factors, and the photodegradation of the organic active layer is one of them.[49,50] It has been well established that the component has to be protected from the atmosphere;[51] however, the behavior of the active layer materials under illumination and in the absence of oxygen has to be further investigated. Despite the efforts of providing an efficient protection to the solar cell against oxygen and humidity, the photodegradation of the materials cannot be avoided. The direct absorption of UV−vis light by the chromophores of polymeric matrix can be responsible for photophysical processes and direct photochemical reactions. It is well-known that under the impact of light and without involvement of oxygen,[52−55] aromatic polymers for instance can undergo various reactions, involving rearrangement (photo-Fries, Norrish y), chain scissions, or cross-linking. Several experiments have been conducted, involving the artificially accelerated aging of the materials. The data obtained from these experiments suggest that, if well protected of oxygen (encapsulation), this active layer is photochemically stable for several years in real conditions of aging.[56]

Experimental Section

Reagents and Solvents. 4-Nitrobenzyl cyanide was synthesized from the nitration of benzyl cyanide with concentrated nitric and sulfuric acid.[57] It was recrystallized from ethanol. 1,4-Divinyl-2,5-bis(hexyloxy)benzene was prepared by Stille coupling reaction[58] of 1,4-dibromo-2,5-bis(hexyloxy)benzene with tributylvinyltin.[59] *N*,*N*-Dimethylformamide (DMF) and tetrahydrofuran (THF) were dried by distillation over CaH_2. Triethylamine was purified by distillation over KOH. All other reagents and solvents were commercially purchased and were used as supplied.

Preparation of Compounds and Copolymers. *Copolymer 3*. A flask was charged with a mixture of **2** (0.2315 g, 0.537 mmol), 1,4-divinyl-2,5-bis(hexyloxy)benzene (0.1775 g, 0.537 mmol), $Pd(OAc)_2$ (0.0050 g, 0.022 mmol), P(*o*-tolyl)$_3$ (0.0376 g, 0.124 mmol), DMF (6 mL), and triethylamine (3 mL). The flask was degassed and purged with N_2. The mixture was heated at 90 °C for 24 h under N_2. Then, it was filtered and the filtrate was poured into methanol. The precipitate was filtered and washed with methanol. The crude product was purified by dissolving in THF and precipitating into methanol (0.2673 g, yield 83%). FT-IR (KBr, cm^{-1}): 3028, 1592, 1506 (aromatic); 1690 (formyl); 2952, 2924 (C−H stretching of hexyloxy chains); 1284, 1210 (ether bond); 1314 (C−N stretching of triphenylamine); 964 (trans vinylene bond). ^{1}H NMR ($CDCl_3$) ppm: 10.01 (s, 1H, formyl); 7.87 (m, 2H, triphenylamine ortho to formyl); 7.35 (m, 4H, triphenylamine ortho to vinylene); 7.11 (m, 10H, vinylene and triphenylamine ortho to nitrogen); 6.75 (s, 2H, phenylene ortho to oxygen); 3.96 (m, 4H, $OCH_2(CH_2)_4CH_3$); 1.81 (m, 4H, $OCH_2CH_2(CH_2)_3CH_3$); 1.37 (m, 12H, $O(CH_2)_2(CH_2)_3CH_3$); 0.91 (t, 6H, $O(CH_2)_5CH_3$). Anal. Calcd for $(C_{41}H_{45}NO_3)_n$: C, 82.10; H, 7.56; N, 2.34. Found: C, 81.94; H, 7.48; N, 2.27.

*Copolymer **P1***. A flask was charged with a solution of **3** (0.3214 g, 0.537 mmol of the repeating unit) and 4-nitrobenzyl cyanide (0.869 g, 0.537 mmol) in a mixture of ethanol (15 mL) and chloroform ((10 mL). Sodium hydroxide (0.18 g, 4.50 mmol) dissolved in ethanol (5 mL) was added portionwise to the stirred solution. The mixture was stirred for 1 h at room temperature under N_2 and then was concentrated under reduced pressure. The concentrate was cooled in a refrigerator to precipitate a dark-green solid. It was filtered, washed thoroughly with water, and dried to afford **P1**. The crude product was purified by dissolving in THF and precipitating into methanol (0.2950 g, 74%). FT-IR (KBr, cm^{-1}): 3030, 1590, 1502, 1452 (aromatic); 2954, 2922 (C−H stretching of hexyloxy chains); 2186 (cyano); 1530, 1346 (nitro); 1286, 1212 (ether bond) and 962 cm^{-1} (trans vinylene bond). ^{1}H NMR ($CDCl_3$) ppm: 8.22 (m, 2H, phenylene ortho to nitro); 7.72 (s, 1H, cyanovinylene); 7.47 (m, 2H, phenylene meta to nitro); 7.34 (m, 6H, triphenylamine meta to nitrogen); 7.10 (m, 10H, vinylene and triphenylamine ortho to nitrogen); 6.74 (s, 2H, phenylene ortho to oxygen); 3.96 (m, 4H, $OCH_2(CH_2)_4CH_3$); 1.81 (m, 4H, $OCH_2CH_2(CH_2)_3CH_3$); 1.36 (m, 12H, $O(CH_2)_2(CH_2)_3CH_3$); 0.92 (t, 6H, $O(CH_2)_5CH_3$). Anal. Calcd for $(C_{49}H_{49}N_3O_4)_n$: C, 79.11; H, 6.64; N, 5.65. Found: C, 78.83; H, 6.75; N, 5.54.

Compound 7. A flask was charged with a solution of **6** (0.3300 g, 1.130 mmol) and 4-nitrobenzyl cyanide (0.3666 g, 2.260 mmol) in ethanol (20 mL). Sodium hydroxide (0.60 g, 16.70 mmol) dissolved in ethanol (10 mL) was added portionwise to the stirred solution. The mixture was stirred for 1 h at room temperature under N_2 and then was concentrated under reduced pressure. The concentrate was cooled in a refrigerator to precipitate a dark-green solid. It was filtered, washed thoroughly with water, and dried to afford **7**. It was purified by column chromatography, eluting with a mixture of dichloromethane and hexane (1:1) (0.54 g, 83%). FT-IR (KBr, cm^{-1}): 1596, 1490 (aromatic); 2162 (cyano); 1522, 1346 (nitro). ^{1}H NMR ($CDCl_3$) ppm: 8.19 (m, 4H, phenylene ortho to nitro); 7.70 (s, 2H, cyanovinylene); 7.50 (m, 4H, phenylene meta to nitro); 7.22 (s, 2H, phenylene ortho to bromine). Anal. Calcd for $C_{24}H_{12}Br_2N_4O_4$: C, 49.68; H, 2.08; N, 9.66. Found: C, 49.34; H, 2.13; N, 9.75.

*Copolymer **P2***. This copolymer was synthesized in 78% yield by reacting **7** with 1,4-divinyl-2,5-bis(hexyloxy)benzene in DMF in the presence of $Pd(OAc)_2$, P(*o*-tolyl)$_3$ and triethylamine according to the procedure described for copolymer **3**. FT-IR (KBr, cm^{-1}): 3060, 1594, 1492, 1453 (aromatic); 2952, 2926 (C−H stretching of hexyloxy chains); 2162 (cyano); 1522, 1346 (nitro); 1290, 1206 (ether bond); 963 (trans vinylene bond). ^{1}H NMR ($CDCl_3$) ppm: 8.20 (m, 4H, phenylene ortho to nitro); 7.70 (s, 2H, cyanovinylene); 7.50 (m, 4H, phenylene meta to nitro); 7.25 (s, 2H, phenylene ortho to cyanovinylene); 7.12 (s, 4H, vinylene); 6.80 (s, 2H, phenylene ortho to oxygen); 3.96 (m, 4H, $OCH_2(CH_2)_4CH_3$); 1.82 (m, 4H, $OCH_2CH_2(CH_2)_3CH_3$); 1.35 (m, 12H, $O(CH_2)_2(CH_2)_3CH_3$); 0.93 (t, 6H, $O(CH_2)_5CH_3$). Anal. Calcd for $(C_{46}H_{44}N_4O_6)_n$: C, 73.78; H, 5.92; N, 7.48. Found: C, 73.51; H, 6.07; N, 7.39.

Scheme 1. Synthesis of Copolymer P1

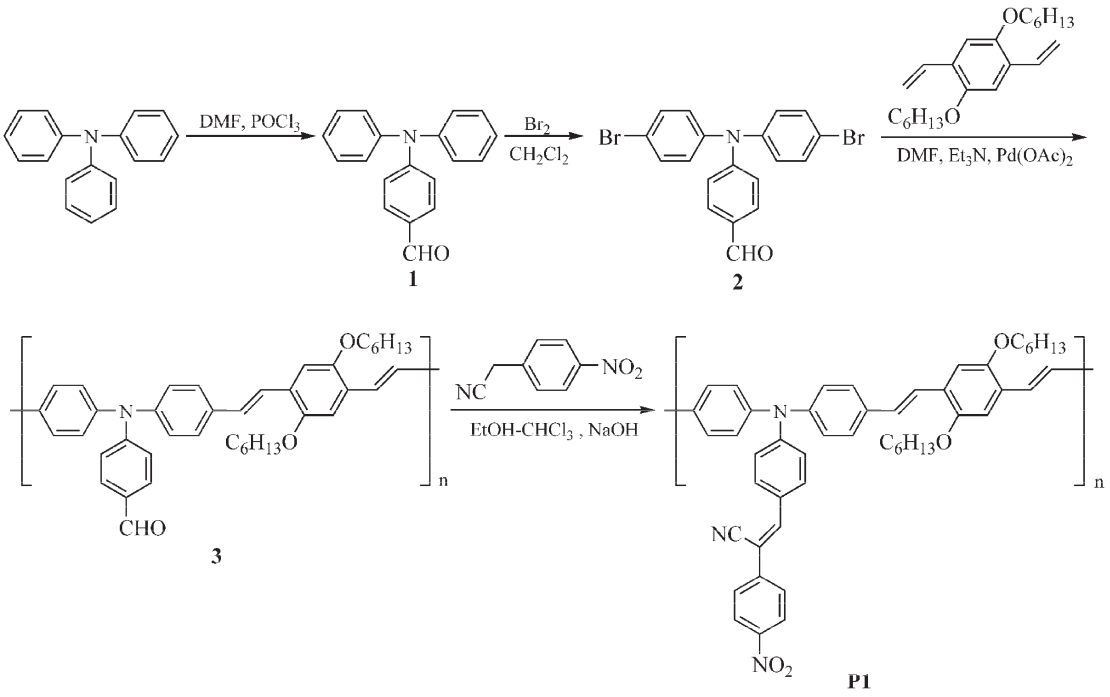

Characterization Methods. IR spectra were recorded on a Perkin-Elmer 16PC FT-IR spectrometer with KBr pellets. ^{1}H NMR (400 MHz) spectra were obtained using a Bruker spectrometer. Chemical shifts (δ values) are given in parts per million with tetramethylsilane as an internal standard. UV−vis spectra were recorded on a Beckman DU-640 spectrometer with spectrograde THF. Elemental analyses were carried out with a Carlo Erba model EA1108 analyzer.

Cyclic voltammetry experiment was carried out on a potentiostat/galvanostat in an electrolyte solution of 0.1 M tetrabutylammonium hexafluorophosphate (Bu_4NPF_6) in dichloromethane, using a three-electrode cell with a gold working electrode, a platinum wire counter electrode, and Ag/Ag^+ (0.01 M) reference electrode. Copolymers to be measured were coated by drop-casting on the gold working electrode from its THF solution.

X-ray diffraction experiments were performed on a Bruker D8 advanced model diffractometer with Cu Kα radiation (λ = 1.542 Å) at a generator voltage 40 kV and current of 40 mA. Atomic force microscopy (AFM) studies were performed using digital instrument nanoscope in trapping mode.

Device Fabrication and Characterization. The copolymer photovoltaic (PV) devices were prepared in a glovebox on indium tin oxide (ITO)-coated glass substrates. The substrates were cleaned in an ultrasonic bath with water and acetone. Poly(3,4-ethylenedioxythiophene):poly(styrenesulfonate) (PEDOT:PSS) was deposited by spin-coating at 3000 rpm for 60 s and baked for 30 min at 80 °C, as hole transport layer. The thickness of PEDOT:PSS layer is about 50 nm. In the glovebox, a mixture of copolymer:PCBM (1:1 ratio) was dissolved in THF and spin-coated on the top of ITO/PEDOT:PSS film at 2000 rpm for 60 s. The thickness of the active layer was 70−80 nm. Finally, aluminum (Al) electrode was thermally evaporated through a shadow mask under high vacuum. The active area of the device is 5 mm^2. The thermal annealing of the active blend layers was carried out at 100 °C for 2 min on the hot plate before the deposition of the Al electrode.

The $J-V$ characteristics of the devices in the dark and under illumination were measured by a semiconductor parameter analyzer (Keithley 4200-SCS). A xenon light source (Oriel) was used to give a simulated irradiance of 100 mW/cm^2 (equivalent to AM1.5 irradiation) at the surface of the device. The photoaction spectrum of the devices was measured using a monochromator (Spex 500 M), and the resulting photocurrent was measured with a Keithley electrometer (model 6514), which is interfaced to the computer by LABVIEW software. We have prepared separate hole and electron only devices having structure ITO/PEDOT:PSS/copolymer:PCBM/Au and Al/copolymer:PCBM/Al, respectively, to measure the hole and electron mobility in the BHJ active layer.

Results and Discussion

Synthesis and Characterization. Copolymer **P1** was synthesized by a four-step reaction sequence which is outlined in Scheme 1. In particular, compounds **1**[60] and **2**[60] were synthesized according to the literature. The Heck reaction of **2** with 1,4-divinyl-2,5-bis(hexyloxy)benzene gave copolymer **3**. This reaction took place in DMF utilizing Et_3N as acid scavenger and $Pd(OAc)_2$ as catalyst. Finally, **3** reacted with 4-nitrobenzyl cyanide in EtOH in the presence of NaOH to afford the target copolymer **P1**.

Scheme 2 outlines the five-step reaction synthesis of copolymer **P2**. Specifically, compounds **4**,[61] **5**,[61] and **6**[61] were synthesized according to reported methods. The reaction of **6** with 4-nitrobenzyl cyanide gave **7**. Finally, the latter reacted with 1,4-divinyl-2,5-bis(hexyloxy)benzene to afford **P2**.

Both copolymers were soluble in common organic solvents such as dichloromethane, chloroform, and THF due to the hexyloxy side groups. **P1** displayed higher solubility in these solvents than **P2**. The noncoplanar configuration of triphenylamine of **P1** enhanced its solubility. In contrast, the two cyanovinylene 4-nitrophenyls of **P2** suppressed the solubility of this copolymer. The crude products were purified by dissolution in THF and precipitation into methanol. The copolymers were obtained in 74% and 78% yield and had number-average molecular weight (M_n) of 13 500 and 11 200, by GPC, with a polydispersity of 2.3 and 2.1 for **P1** and **P2**, respectively.

The FT-IR spectra of copolymers showed common absorption bands which for **P1** appeared at 3030, 1590, 1502,

Scheme 2. Synthesis of Copolymer P2

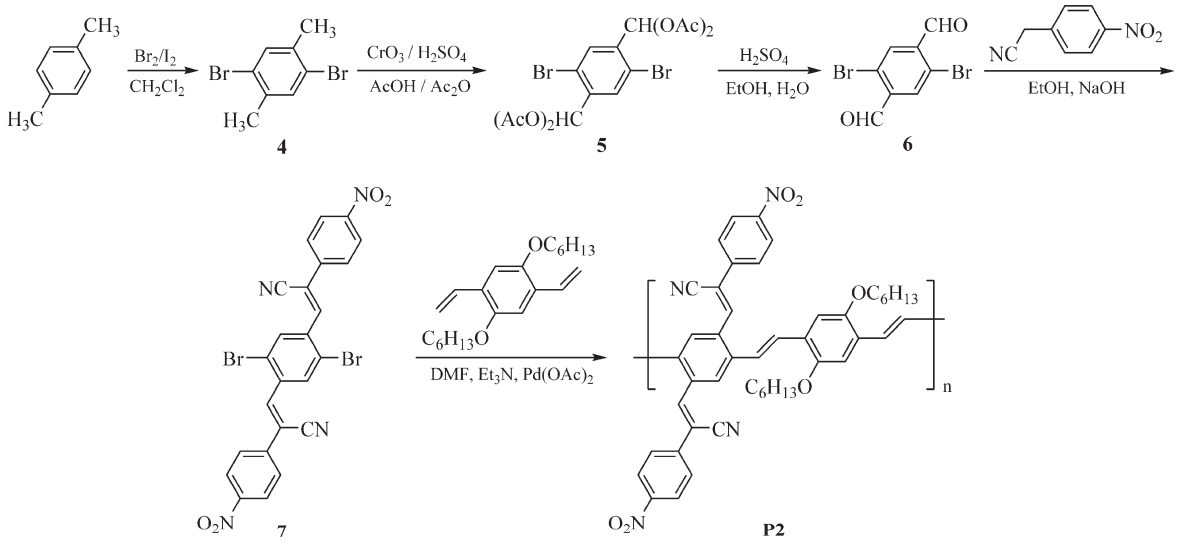

1452 (aromatic); 2954, 2922 (C−H stretching of hexyloxy chains); 2186 (cyano); 1530, 1346 (nitro); 1286, 1212 (ether bond), and 962 cm^{-1} (trans vinylene bond). Figure 1 presents typical ^1H NMR spectrum of **P1**. It displayed an upfield signal at 8.22 ppm assigned to the phenylene "j" ortho to nitro which is deshielded by the nitro group. The cyanovinylene "h" resonated at 7.72 ppm, while the unsubstituted vinylene "f" near 7.10 ppm. The phenylene "i" meta to nitro gave peak at 7.47 ppm, the triphenylamine "f" and "g" at 7.10−7.34 ppm, and the phenylene "e" ortho to oxygen at 6.74 ppm. Finally, the aliphatic "a"−"d" resonated at the region of 0.92−3.96 ppm. The small signals between 5 and 6 ppm are assigned to the terminal vinyl groups $-CH{=}CH_2$.

Photophysical and Electrochemical Properties. Figure 2 presents the UV−vis absorption spectra of copolymers in both dilute (10^{-5} M) THF solution and thin film. Table 1 summarizes the photophysical and electrochemical characteristics of copolymers. The absorption curves were broad and extended from 300 up to ~750 nm in solution and ~800 nm in thin film. **P2** exhibited broader absorption than **P1** in both solution and thin film. The copolymers displayed a short-wavelength absorption maximum ($\lambda_{a,max}$) at the range of 350−400 nm. Besides, they displayed a long-wavelength $\lambda_{a,max}$ at 610−623 nm which is attributable to the intramolecular charge transfer (ICT) between the electron-donating dialkoxyphenylene and/or triphenylamine and the electron-withdrawing cyanovinylene 4-nitrophenyl. The three-dimensional configuration of triphenylamine of **P1** may restrict the π-conjugation along the polymer backbone as well as the ICT. In contrast, **P2** is a fully conjugated copolymer with two electron-withdrawing moieties per repeating unit which favor both π-conjugation and ICT. For this reason, **P2** showed lower optical band gap (E_g^{opt}) than **P1**. Specifically, the thin film absorption onset is located at 739 and 758 nm corresponding to E_g^{opt} of 1.68 and 1.64 eV for **P1** and **P2**, respectively. These E_g^{opt} values are in agreement with those of other related materials containing cyanovinylene 4-nitrophenyls which have been synthesized in our laboratory.[41,42]

Electrochemical cyclic voltammetry is often used to measure the redox properties of the copolymers from which their energy levels of HOMO and LUMO are estimated. The HOMO and LUMO levels are estimated from the onset oxidation (E_{onset}^{ox}) and reduction (E_{onset}^{red}) potentials from the following expressions:[62]

$$E_{HOMO} = -q(E_{ox} + 4.71)\ eV$$

$$E_{LUMO} = -q(E_{red} + 4.71)\ eV$$

The electrochemical data of both copolymers were obtained from the oxidation and reduction voltammograms as shown in Figure 3 and summarized in Table 1. The electrochemical band gap (E_g^{elec}) of both copolymers has also been estimated from the difference between the HOMO and LUMO energy levels and listed in Table 1. The E_g^{elec} values of copolymers are slightly higher than the corresponding optical band gaps, which is probably due to the exciton binding energy of copolymers.[63] It has been generally accepted that an energy difference of 0.3−0.4 eV between the LUMO levels of acceptor and donor materials (i.e., LUMO−LUMO offset) used in BHJ layer is necessary for efficient photoinduced electron transfer from polymer to PCBM.[64] Since the LUMO energy level of PCBM has a value ranging between −4.0 and −4.3 eV,[64] the LUMO−LUMO offset between **P1** or **P2** and PCBM is larger than 0.3 eV, and therefore it is expected that excitons can be easily dissociated at the interface between **P1** or **P2** and PCBM. Furthermore, the HOMO energy levels of **P1** (−5.2 eV) and **P2** (−5.3 eV) are well aligned with the HOMO level of the PEDOT:PSS (−5.1 eV), indicating that holes can be easily transported from the HOMO level of **P1** and **P2** to PEDOT:PSS. Therefore, both copolymers can be used as electron donors with PCBM as electron acceptor for BHJ PV devices.

Electrical and Photovoltaic Properties of Pristine P1 and P2. We have investigated the electrical and photovoltaic properties of single-layer devices based on **P1** or **P2**, before using these materials as donor component for BHJ photovoltaic devices. Figure 4a,b shows the $J-V$ characteristics of the devices based on pristine **P1** and **P2** thin films sandwiched between ITO/PEDOT:PSS and Al electrodes, in dark as well as under illumination intensity of 100 mW/cm^2 at room temperature. The $J-V$ characteristics of both devices in dark show a rectification effect when positive potential is applied to ITO/PEDOT:PSS electrode with respect to the Al electrode. Since the HOMO level of PEDOT:PSS is very close to HOMO levels of both **P1** and **P2**, this electrode behaves as Ohmic contact for hole injection from the PEDOT:PSS-coated ITO electrode into the HOMO of copolymer. However, the LUMO level of both copolymers is very

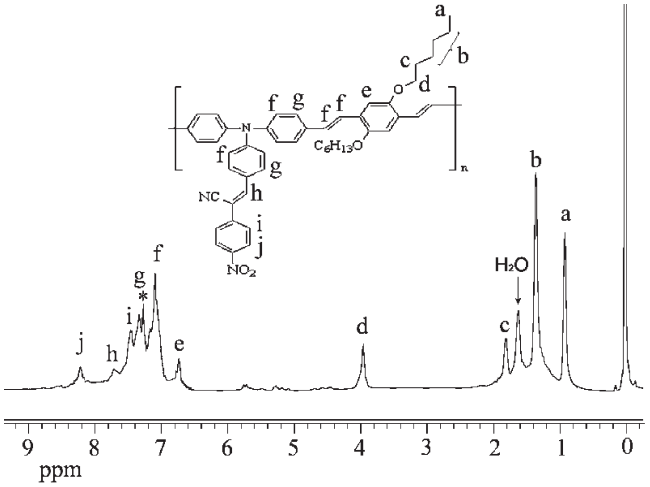

Figure 1. ^{1}H NMR spectrum of copolymer **P1** in $CDCl_3$ solution. The solvent peak is denoted by an asterisk.

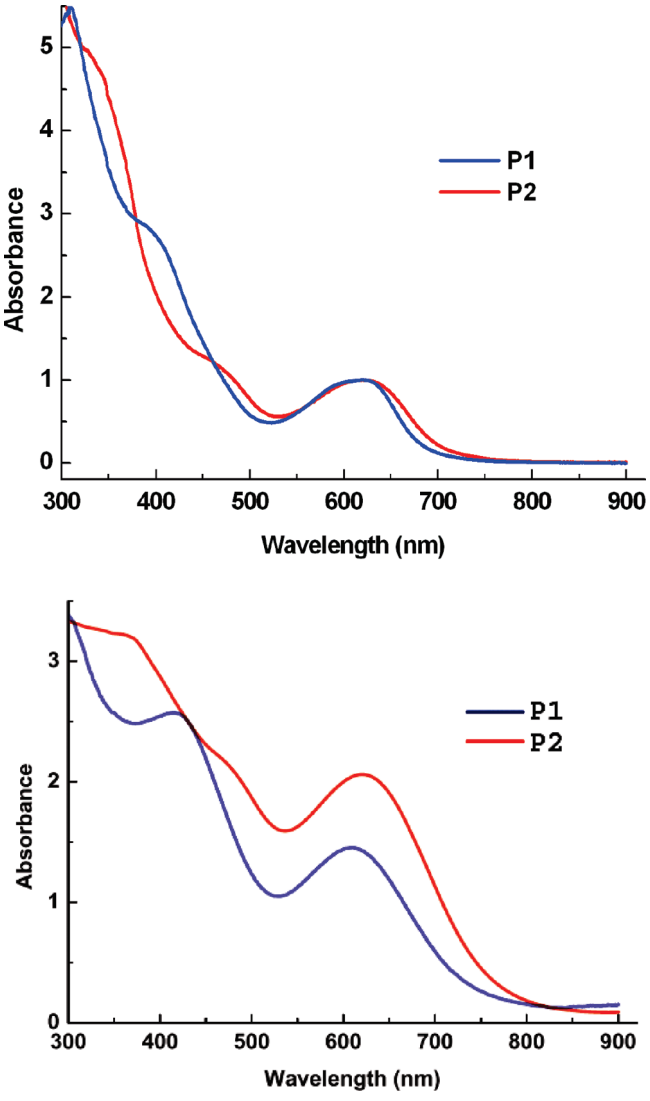

Figure 2. UV−vis absorption spectra of copolymers in THF solution (top) and thin film (bottom).

far from the work function of Al (−4.2 eV) and forms the Schottky barrier for electron injection from Al into the LUMO level of copolymers. Consequently, the rectification effect is due to the formation of the Schottky barrier at the Al−copolymer layer interface.

Table 1. Optical and Electrochemical Properties of Copolymers

copolymer	P1	P2
$\lambda_{a,max}$[a] in solution (nm)	623	623
$\lambda_{a,max}$[a] in thin film (nm)	610	623
thin film absorption onset (nm)	739	758
E_g^{opt}[b] (eV)	1.68	1.64
E_{onset}^{ox} (V)	0.49	0.56
E_{onset}^{red} (V)	−1.26	−1.11
HOMO (eV)	−5.20	−5.30
LUMO (eV)	−3.45	−3.60
E_g^{el}[c] (eV)	1.75	1.70

[a] $\lambda_{a,max}$: the absorption maxima from the UV−vis spectra in THF solution or in thin film. [b] E_g^{opt}: optical band gap determined from the absorption onset in thin film. [c] E_g^{el}: electrochemical band gap determined from cyclic voltammetry.

The charge mobility of the conjugated materials used as photoactive layer in organic PV device is also an important factor, which influences the short circuit current (J_{sc}). The hole mobilities of both copolymers were measured using the space charge limited current (SCLC) method[65] with the device structure ITO/PEDOT:PSS/**P1** or **P2**/Au. The $J-V$ characteristics of the devices were plotted as $\ln[Jd^3/(V_{app} - V_{bi})]$ vs $[(V_{app} - V_{bi})/d]^{1/2}$ (where V_{appl} and V_{bi} is the applied voltage and built-in potential, respectively) and are shown in Figure 5. The hole mobilities of **P1** and **P2** calculated from the intercepts of corresponding lines are 4.5×10^{-5} and 2.1×10^{-5} $cm^2/(V\,s)$ for **P1** and **P2**, respectively. These results indicate that both **P1** and **P2** behave as p-type organic semiconductor with high hole mobility and can be used as electron donor for BHJ devices.

The PV parameters of the devices fabricated with **P1** and **P2** were estimated from the $J-V$ characteristics under illumination, as shown in Figure 4b, and the PV parameters are summarized in Table 2. It can be seen from this table that both J_{sc} and PCE are higher for the device based on **P1** as compared to **P2** under the same conditions. Since the absorption spectra and the band gap of both copolymers are almost the same, the amount of light absorbed by both copolymers will also be almost the same. This implies that the number of excitons generated in the photoactive layer is the same. Therefore, the higher hole mobility of **P1** as compared to **P2**, as described earlier, may be responsible for the higher J_{sc} and PCE. The HOMO level of **P1** is more aligned with the HOMO level of PEDOT:PSS, indicating that holes can be easily transported from **P1** to PEDOT:PSS. However, holes can be trapped at the interface between the **P2** and PEDOT:PSS due to the difference in the HOMO levels of **P2** and PEDOT:PSS, which causes the slight band bending at the interface. This band bending is also responsible for the lower values of V_{oc} for the devices based on **P2** due to the voltage loss across the interface.

Bulk Heterojunction Devices Based on P1 and P2 with PCBM. Before testing the **P1** and **P2** copolymers as electron donor, with PCBM as acceptor for BHJ devices, photoluminescence (PL) measurements were performed to examine the charge transfer efficiency from the copolymer to PCBM. Figure 6 compares the PL spectra of **P1**, **P1**:PCBM, and **P2**:PCBM composite in solid state. **P1** shows strong PL with emission maximum at 815 nm. The intensity of both **P1**:PCBM and **P2**:PCBM is quenched by addition of PCBM, indicating that a photoinduced charge transfer takes place effectively from copolymer to PCBM. The quenching in **P1**:PCBM is higher compared to **P2**:PCBM which indicates that a more efficient charge transfer occurs in former.

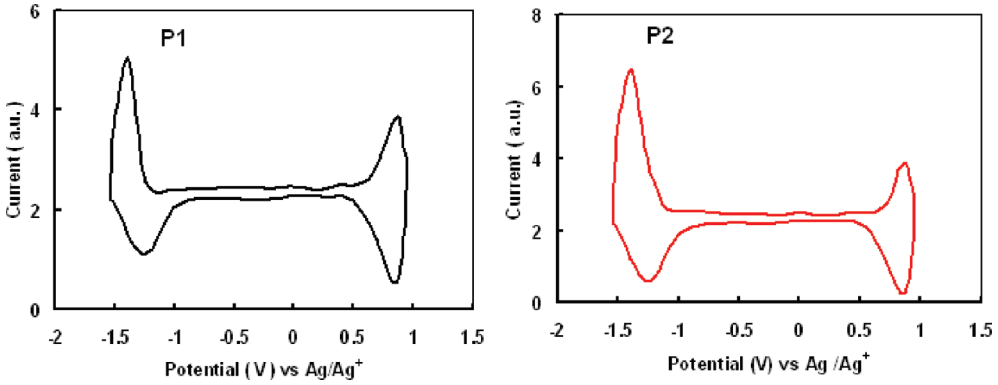

Figure 3. Cyclic voltammogram of **P1** and **P2**.

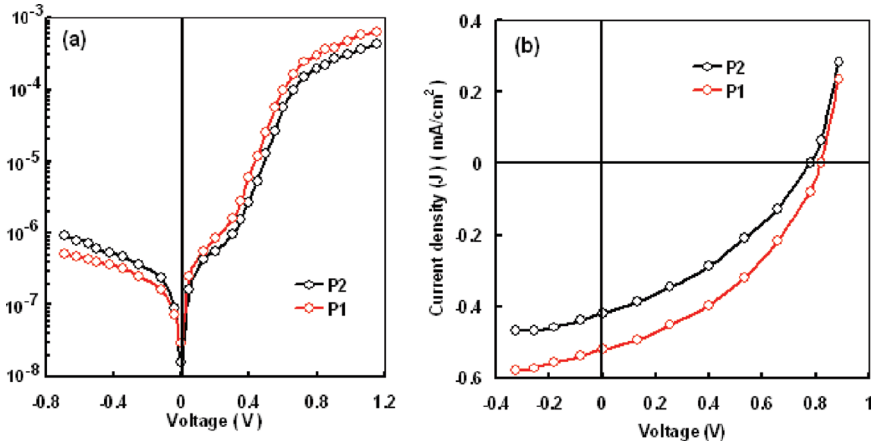

Figure 4. Current−voltage characteristics of the devices based on **P1** and **P2** in dark (a) and under illumination intensity of 100 mW/cm^2 (b).

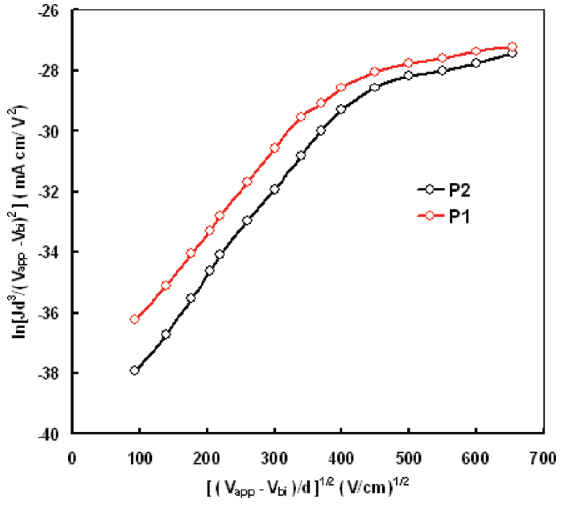

Figure 5. Current−voltage characteristics of ITO/PEDOT:PSS/**P1** or **P2**/Au devices, plotted in the form of $\ln[Jd^3/(V_{app} - V_{bi})^2]$ vs $[(V_{app} - V_{bi})/d]^{0.5}$.

In order to check the PV properties of copolymers **P1** and **P2**, we fabricated polymer solar cells with the architecture ITO/PEDOT:PSS/**P1** or **P2**:PCBM/Al, where both **P1** and **P2** were used as electron donor and PCBM as electron acceptor. The active layer constituted of a copolymer:PCBM blend at various weight ratios, and it was deposited by spin-coating on an ITO glass substrate covered by a PEDOT:PSS layer. We found that the optimum copolymer:PCBM weight ratio was around 1:1.

Table 2. Photovoltaic Parameters of the Devices Based on Pristine P1 and P2 Sandwiched between ITO/PEDOT:PSS and Al Electrodes

copolymer	short-circuit current (J_{sc}) (mA/cm^2)	open-circuit voltage (V_{oc}) (V)	fill factor (FF)	power conversion efficiency (η) (%)
P1	0.52	0.83	0.49	0.21
P2	0.44	0.78	0.45	0.15

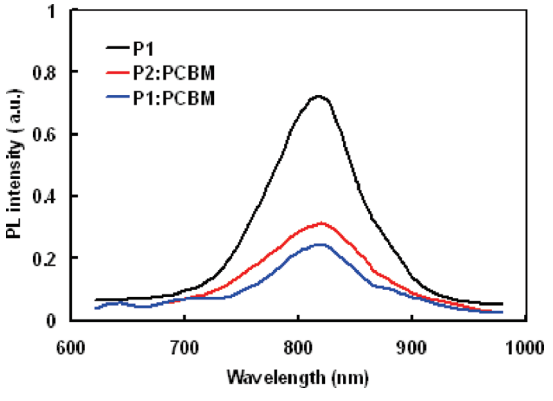

Figure 6. Photoluminescence spectra of **P1**, **P1**:PCBM, and **P2**:PCBM thin films.

The $J-V$ characteristics of the PV devices in dark and under illumination of AM 1.5 (100 mW/cm^2) are shown in Figure 7. Table 3 lists the PV parameters obtained from the $J-V$ characteristics for the best performing devices. The devices fabricated from both copolymers clearly show a

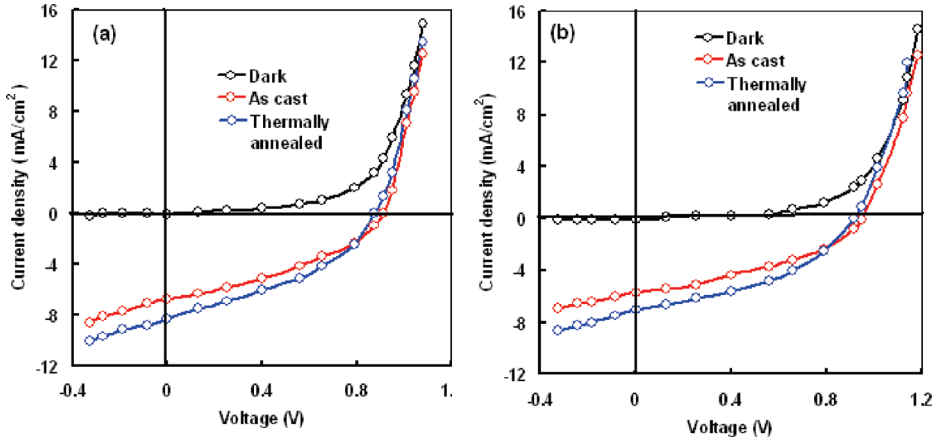

Figure 7. Current−voltage characteristics of the devices based on **P1**:PCBM (a) and **P2**:PCBM (b) in dark and under illumination intensity of 100 mW/cm^2 of the as-cast and thermally annealed layer.

Table 3. Photovoltaic Parameters of the Devices Based on P1:PCBM and P2:PCBM Blend Sandwiched between ITO/PEDOT:PSS and Al Electrodes

copolymer	short-circuit current (J_{sc}) (mA/cm^2)	open-circuit voltage (V_{oc}) (V)	fill factor (FF)	power conversion efficiency (η) (%)
P1:PCBM (as-cast)	6.78	0.91	0.51	3.15
P2:PCBM (as-cast)	5.70	0.95	0.49	2.60
P1:PCBM (annealed)	8.35	0.87	0.56	4.06
P2:PCBM (annealed)	7.00	0.92	0.53	3.35

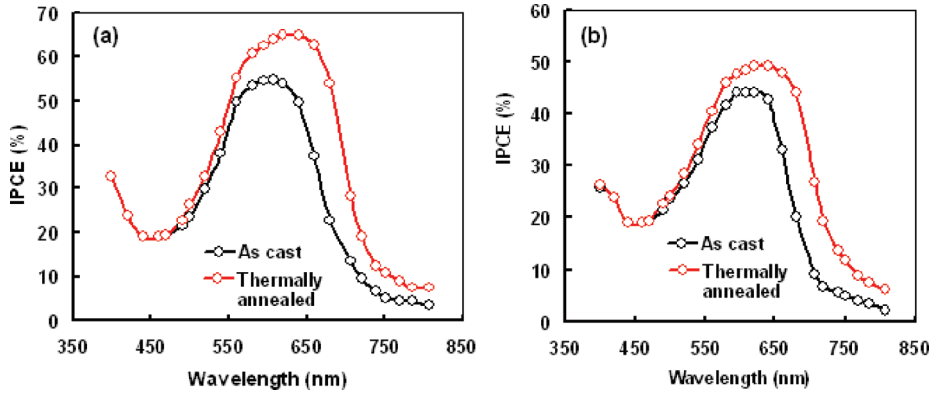

Figure 8. IPCE spectra of the bulk heterojunction photovoltaic devices based on **P1**:PCBM (a) and **P2**:PCBM (b) blends.

rectifying behavior in dark and exhibit significant PV effects under illumination. Our measurements (Table 3) indicate that these devices have a high V_{oc} comparable to that obtained from P3HT:PCBM device (V_{oc} = 0.55−0.60). The slight higher value of V_{oc} for device with **P2**:PCBM as compared to **P1**:PCBM is in agreement with the value of the HOMO levels of **P2** and **P1** (Table 1) since the V_{oc} is related to the energy difference between the LUMO level of acceptor (PCBM) and the HOMO level of the donor (copolymer).[66] It can also be seen that the J_{sc} and PCE of the device based on **P1** is higher than that to **P2**. Furthermore, the device based on **P1** shows an enhanced fill factor of 0.52. The improvement in J_{sc} and PCE could be ascribed to a more efficient charge separation and transport between **P1** and PCBM. Upon comparing, this result could be attributed to the higher energy difference in the LUMO levels of **P1** and PCBM as compared to that between **P2** and PCBM (Table 1).

The devices were also tested for their incident photon to current efficiency (IPCE). The values of IPCE have been estimated using the following expression:

$$\text{IPCE}\ (\%) = 1240 J_{sc}/\lambda P_{in}$$

where J_{sc} (mA/cm^2) is the short-circuit photocurrent; P_{in} (W/m^2) and λ (nm) are the illumination intensity and wavelength of the monochromatic light, respectively. The IPCE spectra of the devices (Figure 8) show a peak which corresponds to the absorption band of the respective polymers. The similarity of the absorption spectrum with the IPCE response demonstrates that the excitons produced by the absorption of photons in copolymers are dissociated into free charge carriers in the interfaces between **P1** or **P2** and PCBM in the active layer and subsequently collected by the electrodes. The maximum values of IPCE for **P1**:PCBM and **P2**:PCBM based devices are about 54% and 43%, respectively. The IPCE values are consistent with the relatively higher values of J_{sc} and PCE of the **P1**:PCBM-based BHJ PV device.

The photocurrent in BHJ PV device is determined by the product of the absorbed photons within the solar spectrum and incident quantum efficiency (IQE) of the device.[67] As it can be seen from Table 1 and Figure 2, the optical absorption spectra and band gap of both copolymers are almost similar, indicating that the number of the photons absorbed by the active layer used in both devices is also almost the same. Therefore, the difference in photocurrent in the present

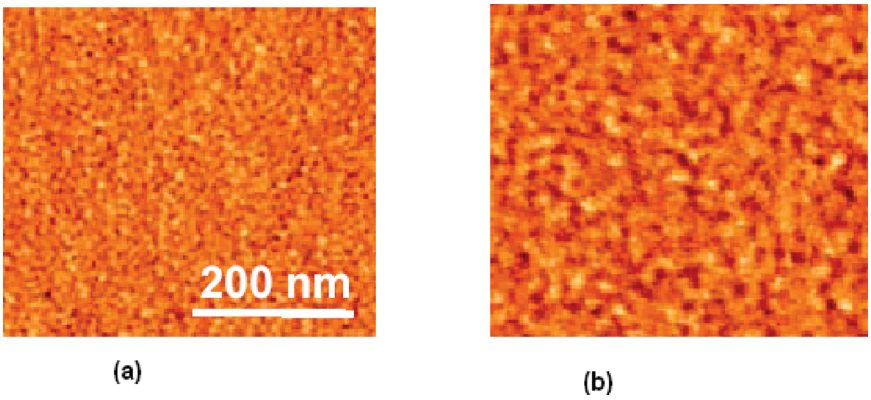

Figure 9. AFM images of **P1**:PCBM blend thin films as cast (a) and thermally annealed (b) films.

devices is attributed to the difference between the IQE of the devices. The IQE is determined by three processes: (a) migration and diffusion of photogenerated excitons toward the D/A interface, (b) exciton dissociation and charge separation at the interfaces, and (c) collection of charge carriers by the collecting electrodes. The process "a" depends upon the nanoscale phase separation between the donor and acceptor materials used in the BHJ active layer. The AFM images of the **P1**:PCBM and **P2**:PCBM are similar, which indicates that both blends have the same nanoscale phase separation. For process "b", a sufficient large energy difference between the LUMO of donor and acceptor material is required for ultrafast photoinduced charge transfer. As can be seen from Table 1, this difference is higher for **P1**:PCBM as compared to **P2**:PCBM, resulting in higher IQE for the device based on the former blend. The process "c" depends upon the percolated path of electrons and holes in the BHJ active layer and also on the position of HOMO and LUMO levels of donor and acceptor materials, respectively, relative to the work function of anode and the cathode. The HOMO level of **P1** is closer to the HOMO level of PEDOT:PSS, which results in a more efficient collection of holes. Therefore, processes "b, c" are responsible for the higher value of J_{sc} and PCE of the device fabricated with **P1**:PCBM blend. The hole mobility for **P1** is higher than that for **P2** which leads to the enhanced PCE for this device.

We have also investigated the effect of thermal annealing on the PV response of the BHJ devices using both **P1** and **P2**. The $J-V$ characteristics under illumination and IPCE spectra of the devices are shown in Figures 7 and 8, respectively. The overall PCE for the devices based on thermally annealed **P1** and **P2** are 4.06% and 3.35%, respectively. The increase in the IPCE and J_{sc} of the devices based on the thermally annealed blends is attributed to the increase in the crystallinity of the blend and the hole mobility in the copolymer phase upon thermal annealing. This can be ascribed to an effective formation of phase-separated structure induced by thermal annealing, which leads to a better connectivity of each phase.

Charge carrier mobilities in donor−acceptor BHJ thin films play an important role on the performance of the organic PV devices. After the photoinduced charge transfer at the D−A interfaces presented in the bulk of the photoactive layer of the devices, the electrons are localized in the PCBM phase and holes remain in the copolymer phase, i.e., **P1** or **P2** in the present cases. Subsequently, the free electrons and holes must be transported via percolated PCBM and copolymer pathways toward Al and PEDOT:PSS/ITO electrodes, respectively, in order to produce the photocurrent. Therefore, the electron transport in PCBM and hole transport in copolymer are crucial for understanding the photogeneration process in BHJ devices. We have also investigated the effect of thermal annealing on the charge carrier mobility as reported earlier in the literature for P3HT:PCBM blends. The electron and hole mobilities in the BHJ thin film layer can be determined from the $J-V$ measurements using appropriate electrodes which suppress the injection of either electrons or holes, resulting in hole and electron only devices, respectively. We have measured the dark $J-V$ characteristics of **P1**:PCBM blends for hole only and electron only devices using both as cast and thermally annealed blends. We have used devices having ITO/PEDPOT:PSS/ **P1**:PCBM/Au and Al/**P1**:PCBM/Al structure for the estimation of hole mobility and electron mobility, respectively. The charge carrier mobilities of both **P1**:PCBM and **P2**:PCBM blend films were evaluated by space charge limited current (SCLC) measurements.[65] The hole mobilities for both the as cast **P1**:PCBM and **P2**:PCBM are quite comparable with the value measured for pristine copolymers. However, the values of hole mobilities are about 1.3×10^{-4} and 8.4×10^{-5} $cm^2/(V\ s)$ for the annealed **P1**:PCBM and **P2**:PCBM, respectively. The electron mobility for the as-cast and annealed blends is almost the same. The enhanced hole mobility leads to a balanced charge transport in the BHJ PV device.

We have also investigated the morphologies of **P1**:PCBM and **P2**:PCBM blends to get information about the average surface roughness for the film, using atomic force microscopy (AFM). The AFM images for the as-cast and thermally annealed **P1**:PCBM blends are shown in Figure 9. Similar images have been also obtained for **P2**:PCBM. The as-cast **P1**:PCBM blend forms smooth film with an average surface roughness 1.2 nm. Upon thermal annealing of the **P1**:PCBM film at 100 °C, the average surface roughness increases to ~1.8 nm. It can be seen from these images that thermal annealing results in significant changes in the surface morphology. The surface domain size has also been increased upon thermal annealing. This indicates that both the increased domain size and average surface roughness result in an improvement in the crystallinity of the blend, which is responsible for the enhancement in the PCE due to the more efficient photoinduced charge at the D/A interfaces.

Thin film XRD patterns were used to determine the difference in the crystallinity of the **P1**:PCBM blended films (as-cast and thermally annealed) and are shown in Figure 10. Similar results have also been observed for **P2**:CBM. It can be seen in Figure 10 that the as-cast film exhibits a peak centered at $2\theta = 7.8°$, which corresponds to the interplanar distance of 7.8 Å. The thermal annealing leads to higher peak intensity, indicating a higher degree of crystallinity. Since

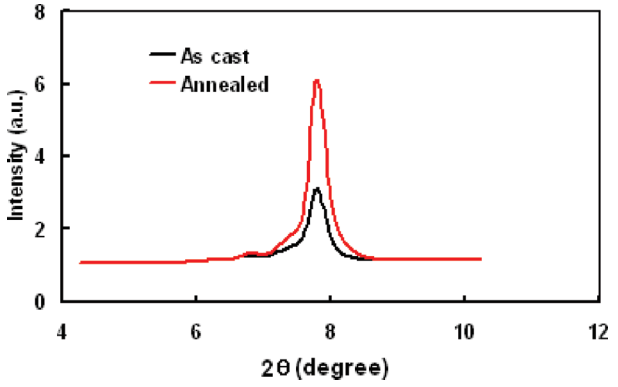

Figure 10. XRD patterns of the as-cast and annealed **P1**:PCBM blend films.

most of the fullerene acceptors, such as PCBM, do not show any diffraction peak in the range of 2θ values used,[68] the change in the crystallinity of the blended thin film after thermal annealing is mainly attributed to an increase in crystalline domains of the copolymer donor material. The increase in the crystalline nature of **P1**:PCBM or **P2**:PCBM after thermal annealing is mainly caused by the copolymer chains self-organization, into an ordered structure, as has been recently reported for P3HT:PCBM blend. The crystallization of copolymer also improves the light-harvesting property by extending the conjugation length.[69] The increase in the crystallinity of copolymer **P1** or **P2** in their respective blends with PCBM upon thermal annealing leads to an improvement in the hole mobility that increases the overall PCE.

Conclusions

Two novel alternating phenylenevinylene copolymers **P1** and **P2** were successfully synthesized. They showed enhanced solubility being soluble in common organic solvents. Their absorption spectra were extended from 300 up to ~750 nm in solution and ~800 nm in thin film, with long-wavelength absorption maximum near 620 nm and optical band gap of 1.64−1.68 eV. The electrochemical data of both **P1** and **P2** indicate that these copolymers are suitable as electron donor with PCBM as acceptor for efficient BHJ PV devices. The BHJ PV devices based on the as cast **P1**:PCBM and **P2**:PCBM show an overall PCE about 3.15% and 2.60%, respectively. The higher values of PCE for the device based on **P1**:PCBM relative to **P2**:PCBM is due to the more efficient photoinduced charge transfer and higher value of hole mobility for **P1**. Further enhancement in PCE (4.06% and 3.35% for **P1**:PCBM and **P2**:PCBM, respectively) with thermally annealed blends is attributed to the increase in hole mobility in the blend due to the improved crystalline nature of the blend. The above results suggest that the balance charge transport and improve crystallinity of the blend are the key factors for efficient collection of charge transport in the PV devices.

References and Notes

(1) Dhanabalan, A.; van Duren, J. K. J.; van Hal, P. A.; van Dongen, J. L. J.; Janssen, R. A. J. *Adv. Funct. Mater.* **2001**, *11*, 255.
(2) Peumans, P.; Uchida, S.; Forrest, S. R. *Nature* **2003**, *425*, 158.
(3) Schilinsky, P.; Asawapirom, U.; Scherf, U.; Biele, M.; Brabec, C. J. *Chem. Mater.* **2005**, *17*, 2175.
(4) Wienk, M. M.; Kroon, J. M.; Verhees, W. J. H.; Knol, J.; Hummelen, J. C.; van Hal, P. A.; Janssen, R. A. J. *Angew. Chem., Int. Ed.* **2003**, *42*, 3371.
(5) Sariciftci, N. S.; Smilowitz, L.; Heeger, A. J.; Wudl, F. *Science* **1992**, *258*, 1474.
(6) Halls, J. J. M.; Walsh, C. A.; Greenham, N. C.; Marseglia, E. A.; Friend, R. H.; Moratti, S. C.; Holmes, A. B. *Nature* **1995**, *376*, 498.
(7) Yu, G.; Gao, J.; Hummelen, J. C.; Wudl, F.; Heeger, A. J. *Science* **1995**, *270*, 1789.
(8) (a) Kim, J. Y.; Lee, K.; Coates, N. E.; Moses, D.; Nguyen, T. Q.; Danteand, M.; Heeger, A. J. *Science* **2007**, *317*, 222. (b) Cai, W.; Gong, X.; Cao, Y. *Sol. Energy Mater. Sol. Cells* **2010**, *94*, 114. (c) Venkataraman, D.; Yurt, S.; Venkataraman, B. H.; Gavvalapalli, N. *J. Phys. Chem. Lett.* **2010**, *1*, 945.
(9) Chen, H. Y.; Hou, J. H.; Zhang, S. Q.; Liang, Y. Y.; Yang, G. W.; Yang, Y.; Yu, L. P.; Wu, Y.; Li, G. *Nature Photonics* **2009**, *3*, 649.
(10) Park, S. H.; Roy, A.; Beaupre, S.; Cho, S.; Coates, N.; Moon, J. S.; Moses, D.; Leclerc, M.; Lee, K.; Heeger, A. J. *Nature Photonics* **2009**, *3*, 297.
(11) Liang, Y. Y.; Feng, D. Q.; Wu, Y.; Tsai, S. T.; Li, G.; Ray, C.; Yu, L. P. *J. Am. Chem. Soc.* **2009**, *131*, 7792.
(12) Hou, J. H.; Chen, H. Y.; Zhang, S. Q.; Chen, R. I.; Yang, Y.; Wu, Y.; Li, G. *J. Am. Chem. Soc.* **2009**, *131*, 15586.
(13) Scharber, M. C.; Wuhlbacher, D.; Koppe, M.; Denk, P.; Waldauf, C.; Heeger, A. J.; Brabec, C. L. *Adv. Mater.* **2006**, *18*, 789.
(14) van Mullekom, H. A. M.; Vekemans, J. A. J. M.; Havinga, E. E.; Meijer, E. W. *Mater. Sci. Eng., R* **2001**, *32*, 1.
(15) Zhang, F.; Jespersen, K. G.; Björström, C.; Svensson, M.; Andersson, M. R.; Sundström, V.; Magnusson, K.; Moons, E.; Yartsev, A.; Inganäs, O. *Adv. Funct. Mater.* **2006**, *16*, 667.
(16) Andersson, L. M.; Zhang, F.; Inganäs, O. *Appl. Phys. Lett.* **2007**, *91*, 071108.
(17) Slooff, L. H.; Veenstra, S. C.; Kroon, J. M.; Moet, D. J. D.; Sweelssen, J.; Koetse, M. M. *Appl. Phys. Lett.* **2007**, *90*, 143506.
(18) Gadisa, A.; Mammo, W.; Andersson, L. M.; Admassie, S.; Zhang, F.; Andersson, M. R.; Inganäs, O. *Adv. Funct. Mater.* **2007**, *17*, 3836.
(19) Mühlbacher, D.; Scharber, M.; Morana, M.; Zhu, Z.; Waller, D.; Gaudiana, R.; Brabec, C. *Adv. Mater.* **2006**, *18*, 2884.
(20) Zhu, Z.; Waller, D.; Gaudiana, R.; Morana, M.; Mühlbacher, D.; Scharber, M.; Brabec, C. *Macromolecules* **2007**, *40*, 1981.
(21) Peet, J.; Kim, J. Y.; Coates, N. E.; Ma, W. L.; Moses, D.; Heeger, A. J.; Bazan, G. C. *Nature Mater.* **2007**, *6*, 497.
(22) Blouin, N.; Michaud, A.; Leclerc, M. *Adv. Mater.* **2007**, *19*, 2295.
(23) Blouin, N.; Michaud, A.; Gendron, D.; Wakim, S.; Blair, E.; Neagu-Plesu, R.; Belletete, M.; Durocher, G.; Tao, Y.; Leclerc, M. *J. Am. Chem. Soc.* **2008**, *130*, 732.
(24) Park, S. H.; Roy, A.; Beaupre, S.; Cho, S.; Coates, N.; Moon, J. S.; Moses, D.; Leclerc, M.; Lee, K.; Heeger, A. *J. Nature Photonics* **2009**, *3*, 297.
(25) Wong, W.-Y.; Wang, X.-Z.; He, Z.; Djurisic, A. B.; Yip, C.-T.; Cheung, K.-Y.; Wang, H.; Mak, C. S. K.; Chan, W.-K. *Nature Mater.* **2007**, *6*, 521.
(26) Liu, L.; Ho, C.-L.; Wong, W.-Y.; Cheung, K.-Y.; Fung, M.-K.; Lam, W.-T.; Djurisici, A. B.; Chan, W.-K. *Adv. Funct. Mater.* **2008**, *18*, 2824.
(27) Wu, P.-T.; Bull, T.; Kim, F. S.; Luscombe, C. K.; Jenekhe, S. A. *Macromolecules* **2009**, *42*, 671.
(28) Wienk, M. M.; Turbiez, M.; Gilot, J.; Janssen, R. A. *J. Adv. Mater.* **2008**, *20*, 2556.
(29) Chen, C.-P.; Chan, S.-H.; Chao, T.-C.; Ting, C.; Ko, B.-T. *J. Am. Chem. Soc.* **2008**, *130*, 12828.
(30) Wang, E.; Wang, L.; Lan, L.; Luo, C.; Zhuang, W.; Peng, J.; Cao, Y. *Appl. Phys. Lett.* **2008**, *92*, 033307.
(31) Hou, J.; Chen, H.-Y.; Zhang, S.; Li, G.; Yang, Y. *J. Am. Chem. Soc.* **2008**, *130*, 16144.
(32) Liang, Y.; Wu, Y.; Feng, D.; Tsai, S.-T.; Son, H.-J.; Li, G.; Yu, L. *J. Am. Chem. Soc.* **2009**, *131*, 56.
(33) Mei, J.; Ogawa, K.; Kim, Y.-G.; Heston, N. C.; Arenas, D. J.; Nasrollahi, Z.; McCarley, T. D.; Tanner, D. B.; Reynolds, J. R.; Schanze, K. S. *ACS Appl. Mater. Interfaces* **2009**, *1*, 150.
(34) Liang, Y.; Feng, D.; Wu, Y.; Tsai, S.-T.; Li, G.; Ray, C.; Yu, L. *J. Am. Chem. Soc.* **2009**, *131*, 7792.
(35) Huo, L.; Hou, J.; Chen, H.-Y.; Zhang, S.; Jiang, Y.; Chen, T. L.; Yang, Y. *Macromolecules* **2009**, *42*, 6564.
(36) (a) Coakley, K. M.; McGehee, M. D. *Chem. Mater.* **2004**, *16*, 4533. (b) Gónes, S.; Neugebauer, H.; Sariciftci, N. S. *Chem. Rev.* **2007**, *107*, 1324.
(37) (a) Hou, J.; Tan, Z.; Yan, Y.; He, Y.; Yang, C.; Li, Y. *J. Am. Chem. Soc.* **2006**, *128*, 4911. (b) Tu, G.; Bilge, A.; Adamczyk, S.; Forster, M.; Heiderhoff, R.; Balk, L. J.; Muehlbacher, D.; Morana, M.; Koppe, M.; Scharber, M. C.; et al. *Macromol. Rapid Commun.* **2007**, *28*, 1781. (c) Li, Y.; Zou, Y. *Adv. Mater.* **2008**, *20*, 2952.
(38) Brabec, C. J.; Shaheen, S. E.; Winder, C.; Sariciftci, N. S. *Appl. Phys. Lett.* **2002**, *80*, 1288.

(39) Kim, K.; Liu, J.; Namboothiry, M. A. G.; Carroll, D. L. *Appl. Phys. Lett*. **2007**, *90*, 163511.
(40) Liang, Y.; Xu, Z.; Xia, J.; Tsai, S. T.; Wu, Y.; Li, G.; Ray, C.; Yu, L. *Adv. Mater*. **2010**, DOI: 10.1002/adma.200903528.
(41) (a) Mikroyannidis, J. A.; Stylianakis, M. M.; Balraju, P.; Suresh, P.; Sharma, G. D. *ACS Appl. Mater. Interfaces* **2009**, *1*, 1711–1718. (b) Mikroyannidis, J. A.; Stylianakis, M. M.; Suresh, P.; Balraju, P.; Sharma, G. D. *Org. Electron*. **2009**, *10*, 1320–1333. (c) Mikroyannidis, J. A.; Sharma, S. S.; Vijay, Y. K.; Sharma, G. D. *ACS Appl. Mater. Interfaces* **2010**, *2*, 270–278. (d) Mikroyannidis, J. A.; Kabanakis, A. N.; Kumar, A.; Sharma, S. S.; Vijay, Y. K.; Sharma, G. D. *Langmuir*, submitted for publication.
(42) (a) Mikroyannidis, J. A.; Kabanakis, A.; Balraju, P.; Sharma, G. D. *J. Phys. Chem. C*, submitted for publication. (b) Mikroyannidis, J. A.; Tsagkournos, D. V.; Balraju, P.; Sharma, G. D. *Org. Electron*., DOI: 10.1016/j.orgel.2010.05.002.
(43) Pan, Q.; Fang, C.; Zhang, Z.; Qin, Z.; Li, F.; Gu, Q.; Wu, X.; Yu, J. *Opt. Mater*. **2003**, *22*, 45–49.
(44) Hisahiro, H.; Kazumasa, W.; Akira, K. JP 61259256 Nov 17, 1986; JP 04028301 May 14, 1992.
(45) Qiuyu, Z.; Li, Z.; Hepeng, Z.; Junping, Z.; Feige, G. CN 101445589 Jun 3, 2009.
(46) Lungenschmied, C.; Dennler, G.; Neugebauer, H.; Sariciftci, S.N..; Glatthaar, M.; Meyer, T.; Meyer, A. *Sol. Energy Mater. Sol. Cells* **2007**, *91*, 379.
(47) Krebs, F. C.; Norrman, K. *Prog. Photovoltaics: Res. Appl*. **2007**, *15*, 697.
(48) Krebs, F. C.; Spanggaard, H. *Chem. Mater*. **2005**, *17*, 5235.
(49) Krebs, F. C.; Carle, J. E.; Cruys-Bagger, N.; Andersen, M.; Lilliedal, M. R.; Hammond, M. A.; Hvidt, S. *Sol. Energy Mater. Sol.Cells* **2005**, *86*, 499.
(50) Norrman, K.; Krebs, F. C. *Sol. Energy Mater. Sol. Cells* **2006**, *90*, 213.
(51) Krebs, F. C. *Sol. Energy Mater. Sol. Cells* **2006**, *90*, 3633.
(52) Rivaton, A.; Gardette, J.-L.; Angew, D. *Makromol. Chem*. **1998**, *173*, 261–262.
(53) Giancaterina, S.; Rossi, A.; Rivaton, A.; Gardette, J. L. *Polym. Degrad. Stab*. **2000**, *68*, 133.
(54) Rivaton, A.; Gardette, J. L. *Polym. Degrad. Stab*. **1999**, *66*, 385.
(55) Grossetete, T.; Rivaton, A.; Gardette, J. L.; Hoyle, C. E.; Ziemer, M.; Fagerburg, D. R.; Clauberg, H. *Polymer* **2000**, *41*, 3541.
(56) Chambon, S.; Rivaton, A.; Gardette, J.-L.; Firon, M. *Sol. Energy Mater. Sol. Cells* **2008**, *92*, 785–792.
(57) Robertson, G. R. *Org. Synth. Collect*. **1941**, *1*, 396; **1922**, *2*, 57 .
(58) McKean, D. R.; Parrinello, G.; Renaldo, A. F.; Stille, J. K. *J. Org. Chem*. **1987**, *52*, 422.
(59) Peng, Q.; Li, M.; Tang, X.; Lu, S.; Peng, J.; Cao, Y. *J. Polym. Sci., Part A: Polym. Chem*. **2007**, *45*, 1632.
(60) Zhang, Z.-G.; Zhang, K.-L.; Liu, G.; Zhu, C.-X.; Neoh, K.-G.; Kang, E.-T. *Macromolecules* **2009**, *42*, 3104.
(61) Xie, Z.; Yang, B.; Liu, L.; Li, M.; Lin, D.; Ma, Y.; Cheng, G.; Liu, S. *J. Phys. Org. Chem*. **2005**, *18*, 962.
(62) Hou, J.; Tan, Z.; Yan, Y.; He, Y.; Yang, C.; Li, Y. *J. Am. Chem. Soc*. **2006**, *128*, 4911.
(63) Zhu, Y.; Chempion, R. D.; Jeneke, S. A. *Macromolecules* **2006**, *39*, 8712.
(64) Zoombelt, A. P.; Fonrodona, M.; Turbiez, M. G.R.; Wienk, M. M.; Janssen, R. A. J. *J. Mater. Chem*. **2009**, *19*, 5336.
(65) (a) Chirvase, D.; Chiguvare, Z.; Knipper, M.; Parisi, J.; Dyakonov, V.; Hummelen, J. C. *J. Appl. Phys*. **2003**, *93*, 3376. (b) Malliaras, G. G.; Salem, J. R.; Brock, P. J.; Scott, C. *Phys. Rev. B* **1998**, *58*, R13411.
(66) (a) White, M. S.; Olson, D. C.; shaheen, S. E.; Kopidakis, N.; Ginley, D. S. *Appl. Phys. Lett*. **2006**, *89*, 143517. (b) Irwin, M. D.; Buchholz, D. B.; Hains, A. W.; Chang, R. P. H.; Marks, T. J. *Proc. Natl. Acad. Sci. U.S.A*. **2008**, *105*, 2783.
(67) (a) Lloyd, M. T.; Anthony, J. E.; Malliaras, G. G. *Mater. Today* **2007**, *10*, 34. (b) Schilinsky, R.; Waldauf, C.; Brabec, C. J. *Appl. Phys. Lett*. **2002**, *81*, 3885. (c) Hoppe, H.; Sariciftci, N. S. *J. Mater. Res*. **2004**, *19*, 1924.
(68) Chikamatsu, M.; Nagamatsu, S.; Yoshida, Y.; Satio, K.; Yase, K. *Appl. Phys. Lett*. **2005**, *87*, 203504/1.
(69) (a) Thompson, B. C.; Frechet, J. M. J. *Angew. Chem., Int. Ed*. **2006**, *47*, 58. (b) Jo, J.; Kim, S.-S.; Na, S.-I.; Yu, B.-K.; Kim, D.-Y. *Adv. Funct. Mater*. **2009**, *19*, 866.